ISSN 2517-7516, Membranes and Membrane Technologies, 2021, Vol. 3, No. 4, pp. 206–211. © Pleiades Publishing, Ltd., 2021.
Russian Text © The Author(s), 2021, published in Membrany i Membrannye Tekhnologii, 2021, Vol. 11, No. 4, pp. 235–241.

Effect of Functional Phosphonic Groups Grafted on the Silica Surface on the Properties of Hybrid Membranes Based on Polybenzimidazole PBI-O-PhT

A. A. Lysova[a], *, I. I. Ponomarev[b], and A. B. Yaroslavtsev[a]

[a] *Kurnakov Institute of General and Inorganic Chemistry, Russian Academy of Sciences, Moscow, 119991 Russia*
[b] *Nesmeyanov Institute of Organoelement Compounds, Russian Academy of Sciences, Moscow, 119334 Russia*
**e-mail: ailyina@yandex.ru*

Received February 24, 2021; revised April 8, 2021; accepted April 9, 2021

Abstract—Hybrid membranes based on polybenzimidazole PBI-O-PhT with incorporated particles of silicon dioxide functionalized with phosphonic groups have been synthesized. The membranes have been prepared in situ by casting a polymer solution with a precursor for particle synthesis. The precursor was a mixture of tetraethoxysilane and (2-diethylphosphatoethyl)triethoxysilane. The mass concentration of the dopant was 5 or 10 wt %, and the mole fraction of functional groups on the oxide surface was varied in the range of 0–100 mol % by changing the composition of the precursor mixture. The resulting membranes have been characterized using transmission and scanning electron microscopy, IR spectroscopy, and impedance spectroscopy. Grafting of functional $-PO_3H_2$ groups onto the silica surface leads to a significant increase in the uptake of phosphoric acid by hybrid membranes, the content of which determines the functional properties of these materials. An increase in the number of $-PO_3H_2$ groups leads to both an increase in the degree of acid doping and ionic conductivity. The conductivity of the best samples obtained reaches 0.081 S/cm at 160°C. The introduction of acid groups on the dopant surface is a promising approach from the point of view of reducing the amount of phosphoric acid required to maintain a high proton transport rate.

Keywords: hybrid membranes, polybenzimidazole, proton conductivity, silica, surface functionalization
DOI: 10.1134/S2517751621040041

INTRODUCTION

The incorporation of nanosized inorganic particles into ion-exchange polymer membranes to improve their properties and expand the possibilities of their application in high-temperature fuel cells (FCs) is the direction of research in many publications [1–3]. Hybrid nanomaterials in many cases demonstrate a significant improvement in a number of important properties in comparison with an undoped polymer because of the presence of nanoparticles in the membrane matrix [4]. Among various types of nanosized inorganic dopants, which include heteropoly acids, carbon nanotubes, zeolites, fullerenes, graphene, inorganic salts and oxides, and many others, silica nanoparticles attract considerable attention due to their high surface area, large pore volume, high mechanical and thermal stability, and ease of surface functionalization [5–13].

The distribution of dopant particles in the polymer matrix makes a significant contribution to the properties of composite materials [14]. Nanosized silica has a strong tendency toward aggregation, and the homogeneous distribution of nanoparticles in the polymer matrix is a key problem in the creation of hybrid membranes [5]. In this context, the in situ method, in which the formation of uniformly distributed inorganic nanoparticles isolated from each other occurs directly in the polymer, is one of the most attractive methods [15].

Surface modification of silica particles with organic groups leads to a change in the interaction between the dopant particles and the polymer matrix. It is very attractive to use dopants with an acidic surface, which make it possible to increase the concentration of carriers, water content, and membrane conductivity [16–18]. To enhance the acidic functions of silica, in some cases, it is sulfonated or grafted with phosphonic acid ($-PO_3H_2$) groups. The introduction of acid groups on the oxide surface not only can increase the conductivity of the hybrid material as a whole lead, but also can decrease gas permeability and improve the mechanical and thermal stability of composite membranes [19–26]. It is noted that the grafting of $-PO_3H_2$ groups is especially important for membranes used under high-temperature and low-humidity conditions [27, 28]. The use of such dopants seems to be especially expedient in the case of polymers based on polybenzimidazoles (PBIs) that are

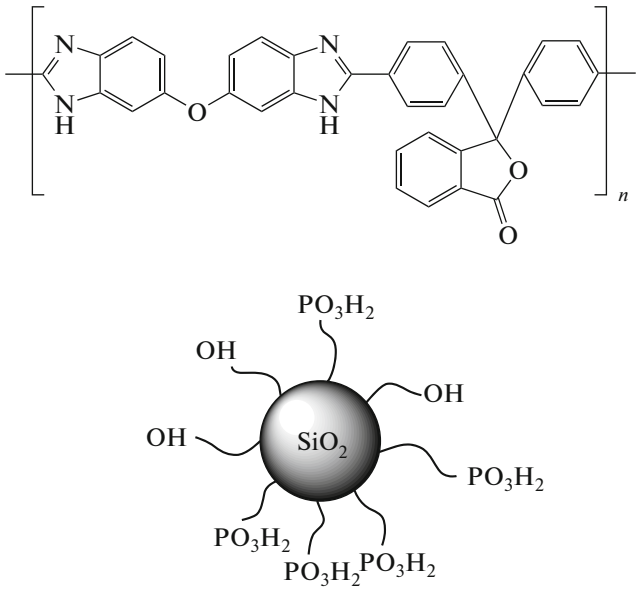

Fig. 1. Schemes of the structure of polybenzimidazole PBI-O-PhT and modified silicon oxide.

doped with phosphoric acid to impart conductivity. However, their conductive properties deteriorate during FC operation because of acid leaching from the polymer in a high-humidity environment. Therefore, it seems interesting to introduce into the membrane $-PO_3H_2$ groups fixed on inorganic supports, for example, on silica [29–33]. We have previously investigated hybrid membranes based on the cardo polymer polybenzimidazole made of 3,3',4,4'-tetraaminodiphenyl oxide and 3,3-bis(*p*-carboxyphenyl)phthalide (PBI-O-PhT), which has high thermal stability, excellent mechanical properties, and chemical and oxidative stability. Silica, zirconia, and silica with grafted sulfo and imidazole functional groups were used as dopants [15, 34, 35].

In this study, we planned to investigate hybrid membranes based on PBI-O-PhT and silica with grafted propylphosphonic groups (Fig. 1). It was of interest to examine the effect of $-PO_3H_2$ groups grafted onto the oxide surface on acid uptake and transport properties of membranes. It was assumed that the introduction of such groups will facilitate the retention of phosphoric acid by the membranes and increase their conductivity.

EXPERIMENTAL

The polymer PBI-O-PhT was synthesized according to the procedure described in [36]. PBI-O-PhT was modified by the in situ method; i.e., by casting a solution containing a precursor for the synthesis of silica with a surface modified with ethylphosphonic groups. For this purpose, a mixture of tetraethoxysilane (TEOS, Aldrich, 98%) and (2-diethylphosphatoethyl)triethoxysilane (TEOS-P, Gelest, 95%) was added to a polymer solution in *N*-methylpyrrolidone (4 g of polymer/100 mL of solvent), in which the TEOS-P mole fraction was 0–100%, and the design mass fraction of the dopant was 5 or 10%. Thereafter, the mixture was homogenized by sonicating for 5 min and then dried on a glass substrate at 50–60°C for 3 days.

To remove the residual solvent, the resulting films were heated in a vacuum at 120°C. Next, the alkoxy groups of silanes and the phosphonic ester group were hydrolyzed in a 12% NH_3 solution (KhimMed, special purity grade) at 25°C for 24 h. Thus, films with silica formed directly in the polymer matrix were obtained. Hereinafter, these samples are designated as PBI/SiP-5-x and PBI/SiP-10-x, where 5 or 10 is the percentage of the dopant in the membrane and **x** is the molar fraction of TEOS-P in the precursor for dopant synthesis, which determines the concentration of phosphonic groups in the dopant.

To impart conducting properties, all the samples were kept for 7 days at 25°C in 75% phosphoric acid (KhimMed, analytical grade). After this procedure, the mass of the membranes increased by a factor of 2.5–3. The resulting materials were dried in a vacuum at 70°C for 4 h and stored in a desiccator over P_2O_5.

Research Methods

The infrared absorption spectra of the samples in the form of thin films were recorded on a Nicolet iS5 Fourier-transform IR spectrometer in the range of 4000–400 cm^{-1}.

The degree of doping of membranes with phosphoric acid (number of H_3PO_4 molecules per repeat unit of the polymer, *n*) was determined based on the mass of absorbed acid according to the procedure described in [37].

The morphology and elemental composition of the membranes were studied by scanning electron microscopy using a Carl Zeiss NVision 40 scanning electron microscope equipped with an Oxford X-Max X-ray spectral detector. The microstructure of the samples was studied using a Jeol JEM 2100 transmission electron microscope.

The dopant content in hybrid membranes was determined by annealing the sample at 800°C until the polymer was completely burned out and weighing the dry residue of the oxide using a Netzsch TG 209 F1 thermal balance with an accuracy of 10^{-6} g.

To determine the ion-exchange capacity of the oxide samples, weighed portions were kept for a week in 40 mL of a 0.5 M aqueous calcium chloride solution for the complete transfer of protons into solution, followed by separation of the precipitate by centrifugation. A 10-mL aliquot was taken from the obtained solutions and titrated with 0.01 M sodium hydroxide solution in the presence of phenolphthalein. In this

way, the ion-exchange capacity of the samples was determined.

Elemental analysis of silica samples was performed using a 4210 MP-AES atomic emission spectrometer. The sample for analysis was prepared by dissolving a weighed portion (about 30 mg) of silica in 1 mL of a 20% hydrofluoric acid solution, followed by multiple dilutions.

Conductivity measurements were carried out using a Z500 PRO impedance meter (Elins, Russia) with graphite electrodes at a frequency of $10^{-2} \times 10^{6}$ Hz in a potentiostatic mode with a sinusoidal signal amplitude of 80 mV. The conductivity was measured in the temperature range from 25 to 160°C with a step of 10–15°C. The value of ionic conductivity was calculated by extrapolating the semicircles of the bulk conductivity component to the active resistance axis. In the calculation, we used the conductivity formula given in [38]. For all the membranes, the proportion of direct-current electron conductivity did not exceed 0.01% of total conductivity.

RESULTS AND DISCUSSION

To assess the amount of functional groups, silicas with grafted moieties outside the membranes were synthesized. In this case, we did not manage to obtain a powdered sample with x = 100 mol %. The most likely reason for the failure is a relatively low degree of oxide polymerization in this case, since silicon dioxide tends to form a three-dimensional framework, whose formation is hindered by the presence of phosphonic groups with the hydrocarbon moiety, which are to be localized on the surface of the particles. The Si : P ratio in the obtained samples turned out to be somewhat lower than that calculated from the stoichiometry of the precursor (Table 1). The reason for this is the occurrence of hydrolysis processes with partial detachment of functional groups. As the number of $-PO_3H_2$ groups increases, the ion-exchange capacity naturally increases, reaching 4.7 mmol/g for the sample synthesized from a mixture with a TEOS-P mole fraction of 75%. This value appeared to be about half the calculated value. The decrease in the ion-exchange capacity relative to the calculated value is associated not only with incomplete hydrolysis of the ester derivative of the phosphonate group, but also with the blocking of functional groups in the bulk of globules, the volume of which was not limited by the membrane matrix in this case. In addition, phosphonic groups are a rather weak acid; therefore, their dissociation and exchange with calcium cations is incomplete. At the same time, the experiments performed confirm the formation of nanoparticles with the phosphonated surface during the hydrolysis of a mixture of TEOS and TEOS-P.

Table 1. Elemental analysis data for modified silicas

x, mol %	Si : P ratio according to elemental analysis data
25	0.19
50	0.37
75	0.51

Figure 2 shows transmission electron microscopy (TEM) images of some membranes. These data confirm the formation in the membrane matrix of nanoparticles of a 5–10 nm size uniformly distributed in the membrane. The introduction of functional groups on the silica surface leads to slight coarsening of the resulting particles.

Energy dispersive analysis of the membrane section confirms the uniform distribution of silicon and phosphorus in the PBI/SiP hybrid membranes (Fig. 3), whereas the membrane containing silica without functional groups naturally lacks phosphorus.

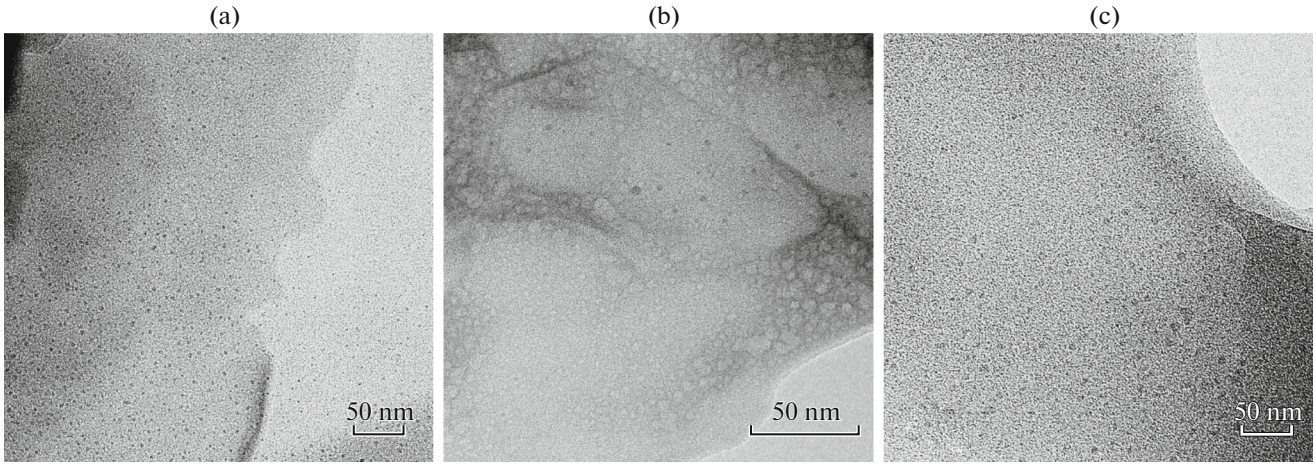

Fig. 2. TEM images of PBI/SiP-5-x samples, where x = (a) 0, (b) 75, or (c) 100 mol %.

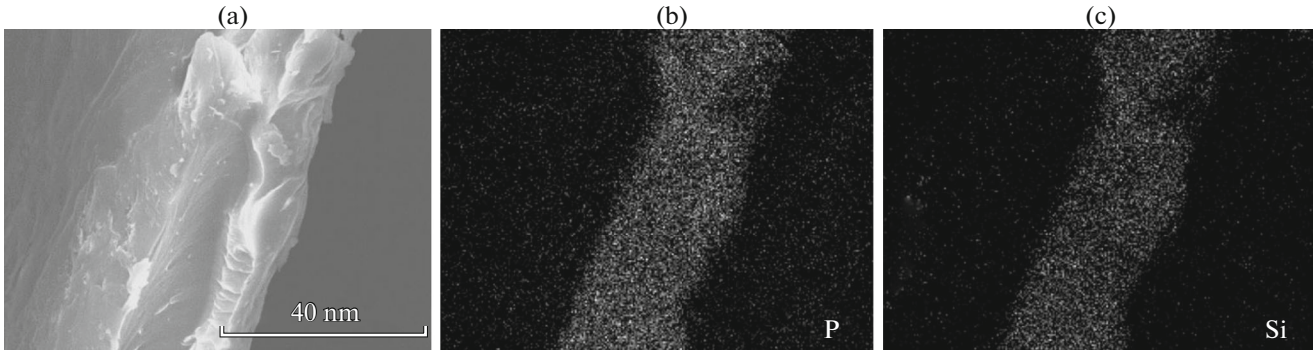

Fig. 3. Electron micrograph and silicon and phosphorus distribution maps in a cut of the PBI/SiP-10-100 membrane.

The dopant content (Table 2) in the membrane was evaluated using thermogravimetry, which comprised weighing the samples before and after annealing at 800°C and calculating the dopant content. The obtained values turned out to be lower than the estimated loading, the discrepancy being primarily due to the difference between the dopant and the annealing product in composition because of the burnout of the grafted groups. Note that the dopant content increases with an increase in the proportion of TEOS-P, approaching the design value. It can be assumed that functional $-PO_3H_2$ groups interact with –NH groups of PBI, immobilizing them in the matrix. Therefore, silica is better retained in the membrane by the hydrolysis of ethoxy groups. The X-ray diffraction pattern of the annealing products is an amorphous halo. The XRD analysis of the elemental composition of some powders obtained by annealing samples with different concentrations of functional groups confirmed that the Si : P ratio increases with an increase in the mole fraction of the groups. For example, it is 1 : 0.54 for the PBI/SiP-10-60 sample and 1 : 0.64 for PBI/SiP-10-100. However, this ratio turns out to be somewhat lower than that for particles obtained outside the membrane, which is associated with the complicated removal of hydrolysis products from the membrane. Thus, the SEM data in combination with the XRD, TEM, and TGA results confirm the incorporation of SiO_2 particles with the phosphonated surface into PBI-O-PhT membranes.

Table 2. Mass fraction of annealed product

Sample	Amount of residue after annealing, wt %
PBI/SiP-5-10	1.5
PBI/SiP-5-30	2.8
PBI/SiP-5-60	4.4
PBI/SiP-5-100	4.6
PBI/SiP-10-10	2.9
ПБИ/SiP-10-30	5.5
PBI/SiP-10-60	7.4
PBI/SiP-10-100	8.4

The hybrid membranes were additionally investigated using IR spectroscopy (Fig. 4). The main spectral changes associated with the introduction of the dopant were observed in the range of 900–1167 cm^{-1}. An increase in absorbance at 1016 cm^{-1} and the appearance of a band at 1046 cm^{-1} are due to asymmetric stretching vibrations in the SiO_4 and PO_3 moieties [39]. There is also an increase in absorbance at 960 and 925 cm^{-1}, which is due to the contribution of symmetric stretching vibrations in the SiO_4 and PO_3 moieties. These data also indicate the presence in the membrane of silica with grafted functional groups.

To convert the membranes into a conductive form, the samples were doped with phosphoric acid. The dependence of the amount of acid absorbed by the membrane on the molar concentration of functional groups in the oxide is shown in Fig. 5. The introduction of functional groups leads to an increase in the uptake of the acid. For the membranes with a dopant content of 10 wt %, its amount increases by ~10% with an increase in the mole fraction of $-PO_3H_2$ groups. An increase in the concentration of $-PO_3H_2$ groups in the dopant facilitates the uptake of a larger amount of acid due to the formation of a system of hydrogen bonds with it.

The dependence of the conductivity of the hybrid membranes on the amount of functional groups on the oxide surface is shown in Fig. 6. The incorporation of the unmodified oxide into the membrane leads to a slight increase in conductivity. However, the grafting of $-PO_3H_2$ groups onto the silica surface significantly changes the situation. Along with an increase in the number of functional groups and, accordingly, in the uptake of phosphoric acid, the conductivity of the membranes also increases significantly, reaching 0.081 S/cm at 160°C (Fig. 6), which is approximately 2.5 times the conductivity of the reference sample. It can be noted that the dependences of the conductivity and the degree of doping on the molar concentration of groups are similar in shape. This resemblance suggests that

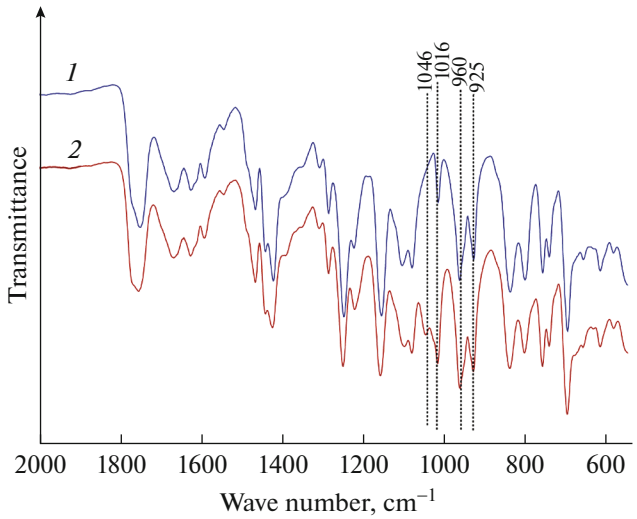

Fig. 4. Fragments of IR spectra of (*1*) PBI and (*2*) hybrid membrane PBI/SiP-10-60.

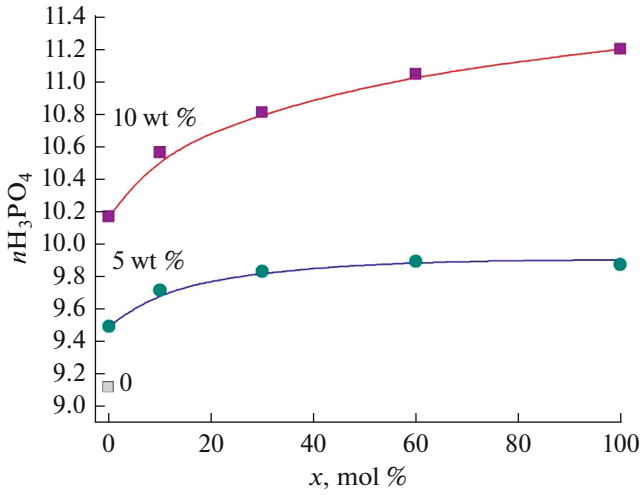

Fig. 5. Dependence of the degree of doping with phosphoric acid (n H_3PO_4) on the mole fraction of functional groups (x) in hybrid membranes; the mass concentration of silica is indicated by numbers in the figure.

the conductivity of these systems is primarily determined by the transport of protons through the system of hydrogen bonds formed by phosphoric acid molecules, the concentration of which in the membrane is much higher. The acidic $-PO_3H_2$ groups of the dopant can also contribute to proton transport. At the same time, at a high concentration of $-PO_3H_2$ groups on the silica surface (10 wt % silica, $x > 60$), the phosphoric acid content in the membrane becomes too high and the membrane plasticizes at high temperatures. Therefore, for hybrid membranes PBI/SiP-10-x at such values of x, the dependence of conductivity on the concentration of functional groups shows a sharp increase at 110°C (Fig. 6, curve *2*) associated with an increase in mobility and "softening" of the entire structure, leading to acceleration of proton transport. At a temperature of 160°C, the PBI/SiP-10-100 membrane loses its mechanical stability; therefore, its conductivity at this temperature is not shown in the figure. At the same time, membranes with PBI/SiP-5-x composition retain their stability over the entire x range.

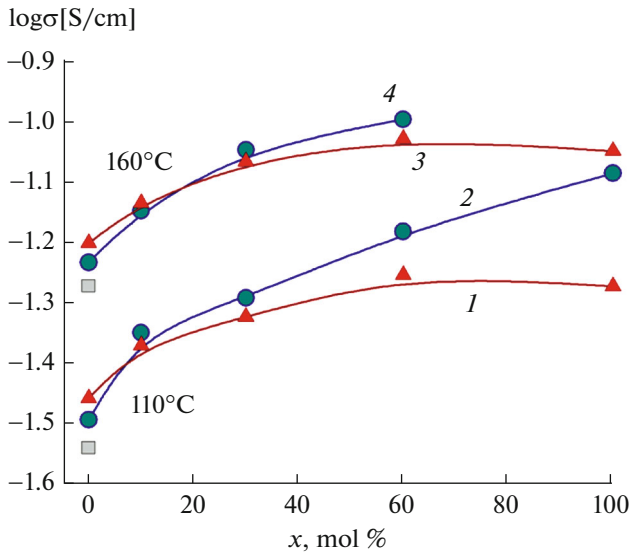

Fig. 6. Dependence of membrane conductivity on the mole fraction (x) of functional groups for (*1*, *3*) PBI/SiP-5-x and (*2*, *4*) PBI/SiP-10-x at (*1*, *2*) 110°C and (*3*, *4*) 160°C. The data points marked with squares (□) refer to the conductivity of the original PBI-O-PhT membrane at 110 and 160°C.

CONCLUSIONS

The study of the hybrid membranes shows that the grafting of functional $-PO_3H_2$ groups onto the silica surface leads to a significant increase in the uptake of phosphoric acid, the concentration of which determines the functional properties of these materials. The conductivity of the best samples reaches 0.081 S/cm at 160°C. At the same time, the polymer plasticizes at high phosphoric acid content. However, due to the contribution of the introduced functional groups to the conductivity, it becomes possible to reduce the amount of introduced acid without a significant loss of conductive properties, which will also contribute to the preservation of mechanical characteristics.

ACKNOWLEDGMENTS

The authors are grateful to Dr. Sci. (Chem.) I.A. Stenina (Kurnakov Institute of General and Inorganic Chemistry, Russian Academy of Sciences) for scanning electron microscopy and Cand. Sci. (Phys.-Math) N.Yu. Tabach-

kova (National Research Technological University MISIS) for transmission electron microscopy measurements.

FUNDING

This work was supported by the Ministry of Education and Science of the Russian Federation within the framework of the State assignment of the Kurnakov Institute of General and Inorganic Chemistry, Russian Academy of Sciences.

REFERENCES

1. C. Y. Wong, W. Y. Wong, K. Ramya, M. Khalid, K. S. Loh, W. R. W. Daud, K. L. Lim, R. Walvekar, and A. A. H. Kadhum, Int. J. Hydrogen Energy **44**, 6116 (2019).
2. J. Escorihuela, J. Olvera-Mancilla, L. Alexandrova, L. F. del Castillo, and V. Compañ, Polymers **12**, 1861 (2020).
3. D. Aili, D. Henkensmeier, S. M. Fernandez, B. Singh, Y. Hu, J. O. Jensen, L. N. Cleemann, and Q. Li, Electrochem. Energ. Rev. **3**, 793 (2020).
4. A. B. Yaroslavtsev, I. A. Stenina, E. Yu. Voropaeva, and A. A. Ilyina, Polym. Adv. Technol. **20**, 566 (2009).
5. S. Ghosh, S. Maity, and T. Jana, J. Mater. Chem. **21**, 14897 (2011).
6. T. Ossiander, C. Heinzl, S. Gleich, F. Schönberger, P. Völk, M. Welsch, and C. Scheu, J. Membr. Sci. **454**, 12 (2014).
7. X. Wang, M. Jin, Y. Li, and L. Zhao, Electrochim. Acta **257**, 290 (2017).
8. S. Maity, S. Singha, and T. Jana, Polymer **66**, 76 (2015).
9. Y. P. Ying, S. K. Kamarudin, and M. S. Masdar, Int. J. Hydrogen Energy **43**, 16068 (2018).
10. D. V. Golubenko, R. R. Shaydullin, and A. B. Yaroslavtsev, Colloid Polym. Sci. **297**, 741 (2019).
11. Y. Zhao, H. Yang, H. Wu, and Z. Jiang, J. Power Sources **270**, 292 (2014).
12. H. Wang, X. Li, X. Zhuang, B. Cheng, W. Wang, W. Kang, L. Shi, and H. Li, J. Power Sources **340**, 201 (2017).
13. K. Oh, O. Kwon, B. Son, D. H. Lee, S. Shanmugam, J. Membr. Sci. **583**, 103 (2019).
14. S. Singha and T. Jana, ACS Appl. Mater. Interfaces **6**, 21286 (2014).
15. A. A. Lysova, P. A. Yurova, I. A. Stenina, I. I. Ponomarev, G. Pourcelly, and A. B. Yaroslavtsev, Ionics **26**, 1853 (2020).
16. E. Yu. Safronova, I. A. Stenina, and A. B. Yaroslavtsev, Russ. J. Inorg. Chem. **55**, 13 (2010).
17. L. G. Boutsika, A. Enotiadis, I. Nicotera, C. Simari, G. Charalambopoulou, E. P. Giannelis, and T. Steriotis, Int. J. Hydrogen Energy **41**, 22406 (2016).
18. E. Gerasimova, E. Safronova, A. Ukshe, Yu. Dobrovolskii, and A. Yaroslavtsev, Chem. Eng. J. **305**, 121 (2016).
19. F. Pereira, K. Vallé, P. Belleville, A. Morin, S. Lambert, and C. Sanchez, Chem. Mater. **20**, 1710 (2008).
20. J. Li, G. Xu, X. Luo, J. Xiong, Z. Liu, and W. Cai, Appl. Energy **213**, 408 (2018).
21. G. He, L. Nie, X. Han, H. Dong, Y. Li, H. Wu, X. He, J. Hua, and Z. Jiang, J. Power Sources **259**, 203 (2014).
22. S.-K. Kim, J. Nanomaterials **2016**, 2954147 (2016).
23. J. Joseph, C.-Y. Tseng, and B.-J. Hwang, J. Power Sources **196**, 7363 (2011).
24. C. Y. Wong, W. Y. Wong, K. Ramya, M. Khalid, K. S. Loh, W. R. W. Daud, K. L. Lim, R. Walvekar, and A. A. H. Kadhum, Int. J. Hydrogen Energy **44**, 6116 (2019).
25. C. Simari, A. Enotiadis, C. L. Vecchio, V. Baglio, L. Coppola, and I. Nicotera, J. Membr. Sci. **599**, 117858 (2020).
26. I. Stenina, D. Golubenko, V. Nikonenko, and A. Yaroslavtsev, Int. J. Mol. Sci. **21**, 5517 (2020).
27. B. Lafitte and P. Jannasch, in *Advances in Fuel Cells*, Eds. K.-D. Kreuer, T. V. Nguyen, and T. Zhao, **Vol. 1** (Elsevier, Oxford, 2007).
28. Y. Zhao, Z. Jiang, D. Lin, A. Dong, Z. Li, and H. Wu, J. Power Sources **224**, 28 (2013).
29. J. Mader, L. Xiao, T. J. Schmidt, and B. C. Benicewicz, Adv. Polym. Sci. **216**, 63 (2008).
30. A. Shabanikia, M. Javanbakht, H. S. Amoli, K. Hooshyari, and M. Enhessari, Electrochim. Acta **154**, 370 (2015).
31. Y. Ozdemir, N. Uregen, and Y. Devrim, Int. J. Hydrogen Energy **42**, 2648 (2017).
32. M. A. Haque, A. B. Sulong, K. S. Loh, E. H. Majlan, and R. E. Rosli, Int. J. Hydrogen Energy **42**, 9156 (2017).
33. A. Kalathil, A. Raghavan, and B. Kandasubramanian, Polym.-Plast. Technol. Mater. **58**, 465 (2019).
34. A. A. Lysova, I. I. Ponomarev, and A. B. Yaroslavtsev, Solid State Ionics **188**, 132 (2011).
35. A. A. Lysova, I. A. Stenina, A. O. Volkov, I. I. Ponomarev, and A. B. Yaroslavtsev, Solid State Ionics **329**, 25 (2019).
36. A. I. Fomenkov, I. V. Blagodatskikh, Iv. I. Ponomarev, Yu. A. Volkova, I. I. Ponomarev, and A. R. Khokhlov, Polym. Sci., Ser. B **51**, 166 (2009).
37. A. A. Lysova, Iv. I. Ponomarev, Yu. A. Volkova, I. I. Ponomarev, and A. B. Yaroslavtsev, Petr. Chem. **58**, 958 (2018).
38. V. I. Volkov, A. V. Chernyak, D. V. Golubenko, V. A. Tverskoy, G. A. Lochin, E. S. Odjigaeva, and A. B. Yaroslavtsev, Membranes (Basel, Switz.) **10**, 272 (2020).
39. G. Socrates, *Infrared and Raman Characteristic Group Frequencies: Tables and Charts*, 3rd Ed. (Wiley, 2004).

Translated by S. Zatonsky